Polarization-independent terahertz three-dimensional subwavelength confinement in coupled slot structures

Joong Wook Lee*[a], Jin-Kyu Yang[b], Jeong Eun Kim[a], Ik-Bu Sohn[a], Hun-Kook Choi[c], Chul Kang[a], and Chul-Sik Kee[a,d]

[a]APRI, Gwangju Institute of Science and Technology (GIST), Gwangju, 500-712, Korea; [b]Department of Optical Engineering, Kongju National University, Kongju, 314-701, Korea; [c]Department of Photonic Engineering, Chosun University, 309 Pilmun-daero, Dong-gu, Gwangju 501-759, Korea; [d]Center for Subwavelength Optics, Seoul, 151-747, Korea

ABSTRACT

We investigate subwavelength confinement of terahertz electromagnetic surface modes in a three-dimensional region with coupled slot structures. Two-dimensional resonance focusing on a subwavelength slot converts to three-dimensional subwavelength confinement, due to sharp edge confinement effect on asymmetric plasmonic structure, at the center position of the slot structures which consists of two or more slots. We also report on the polarization independent confinement of terahertz electromagnetic surface modes beyond diffraction limit. The structure which consists of radially arranged subwavelength slots located at a same center position shows the polarization-independent terahertz three-dimensional subwavelength confinement.

Keywords: terahertz waves, subwavelength confinement, polarization-independent transmission, complicated slot apertures.

1. INTRODUCTION

Focusing and concentrating light on scales much smaller that the wavelength has attracted an exponentially increasing attention for electric, photonic, and biotechnology applications.[1-4] Major applications for realizing the strong light concentration are that they can be applied for the miniaturization of future nanophotonic devices and integrated optical circuits and for the improvement of the spatial resolution and the signal sensitivity of various systems such as spectroscopy, sensing and imaging. Surface plasmon-based circuits have been suggested as a method for solving the size-compatibility problem between electronics and photonics.[5] Individual nanoparticles, which lead to strong field enhancement, have been suggested as a method for probing single molecules and single nanoparticles.[6] These are only a part of feasible applications based on the phenomenon of the strong light concentration on subwavelength scales.

One of major issues in the area is to realize the spatial confinement of electromagnetic energy at terahertz (THz) frequencies.[7] Confining the THz waves into subwavelength area become important for applications requiring highly sensitive detection and highly localized energy.[8-10] Many research groups suggested methods for achieving subwavelength confinement in the THz region. Maier, *et al,* reported that the subwavelength confinement can be realized by periodically structuring the cylindrical surface with grooves on a perfectly conducting wire.[7] The confinement is purely due to the structured surface which generates highly localized surface plasmon polaritons (SPPs). Because of their mimicking characteristics, the localized SPPs is called spoof surface plasmons.[11,12] Seo, *et al*., reported that extremely narrow metallic nano slit results in enormous field enhancement.[13] Here, the metallic nano slit with the gap width less than the skin-depth acts as a nanogap-capacitor charged by light induced currents and thus the field enhancement originates from the edge charge enhanced field at the capacitor-like nanogap. As reducing the gap width, the enhancement therefore increases. We understand that the results show the realization of the extremely strong two-dimensional subwavelength confinement in the subwavelength metallic structures based on the perforated apertures.

The realization of three-dimensional subwavelength confinement in such structures was also expected. Very recently, the three-dimensional subwavelength confinement of THz electromagnetic surface modes was reported in a periodic arrangement of coupled slots perforated on a thin metal film.[14] Here, they explained that the three-dimensional subwavelength confinement originates from carrier concentration on a narrow gap formed by overlapping three slots

Terahertz Emitters, Receivers, and Applications III, edited by Manijeh Razeghi, Alexei N. Baranov, Henry O. Everitt, John M. Zavada, Tariq Manzur, Proc. of SPIE Vol. 8496, 849610 · © 2012 SPIE
CCC code: 0277-786/12/$18 · doi: 10.1117/12.929325

with different angles. They also achieved the tunability in the resonant frequency and the position of the confinement by tuning the structural parameters of the slot length and the intersection position, respectively. This method for realizing the three-dimensional subwavelength confinement has a couple of advantages comparing with other techniques. Comparing with the three-dimensional confinement appearing in the structures based on basic perforated apertures such as a circular hole, this method offers high confinement efficiency and the tunability in the resonant frequency and the position. Even though there exists strong three-dimensional subwavelength confinement appearing in subwavelength cavities, dielectric microspheres, metallic tips, or etc,[15-19] realizing the three-dimensional subwavelength confinement in the structures which consists of the perforated apertures is still important, since those may act as a controllable single *hot hole,* analogues to hot spots due to subwavelength metal particles, on a metal sheet as well as those will be a basic component of plasmonic metamaterials.

Even though we realized the strong three-dimensional subwavelength confinement of the THz electromagnetic surface waves in our previous work,[14] we still feel that the additional functionality such as polarization independence should be added in the structures. In this paper, we report a method for realizing polarization-independent three-dimensional subwavelength confinement of the THz surface waves. We used a coupled slot structure which consists of three perforated slots crossed at a single position to have six-fold rotational symmetry. Basic concept is similar to the case of employing complex apertures such as cross-shaped slots for achieving the polarization independence of extraordinary transmission, perfect absorption, and etc.[20-31] However, the cross-shaped or more complicated structures of the straight slots does not show the three-dimensional subwavelength confinement. We therefore modified the perforated slots to be triangle-shaped. Then we realized both the polarization independence and the three-dimensional subwavelength confinement in the structures.

2. SIMULATIONS AND EXPERIMENTS

We designed the structure, which consists of a periodic arrangement of complex shaped slot apertures, as shown in Fig. 1(a). The structural parameters of a unit cell in the structure are shown in Fig. 1(b). The unit cell consists of three perforated slots with different gap sizes at the center and the edges of each slot. The gap sizes at the edges and the center of each slot are 100 and 10 μm, respectively. The slot therefore looks like a pestle with thin waist. According to the previous researches,[13] as only decreasing the gap size of the slot without changing other structural parameters, the field enhancement factor increases. We therefore expect that the relatively strong field enhancement appears at the center of the slot.

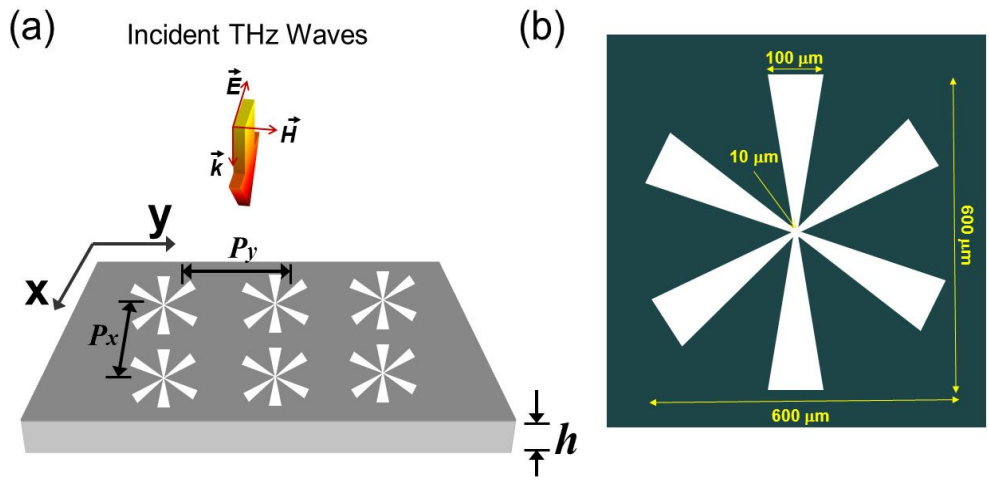

Figure 1. (a) Schematic of the geometry of a sample structure made up of complex slot apertures. The structure consists of a two-dimensional periodic array of the slot apertures perforated on an aluminum film of the thickness of h=10 μm. The periods, Px and Py, along the x and y directions are given by Px=Py=700 μm. The THz waves are normally incident upon the perforated metal surface. (b) Schematic of a unit cell of the structure. The lengths of each slot are L=600 μm. Each slot has different gap sizes at the center and the edges of a slot aperture, which are 10 and 100 μm, respectively.

Three slots are crossed at a single position, as shown in Fig. 2(b), which forms an asterisk-shaped structure with six-fold rotational symmetry. Here the length of all the slots is 600 μm and the period along x- and y-directions is 700 μm. These values were selected to ensure that the localized resonant mode due to the slot aperture is well separated from Wood's anomalies determined by the periodicity of the array of the structure. Rayleigh frequencies for the ± 1 diffraction orders from metal gratings (Wood's anomaly) are given by

$$f_R(\theta) = \frac{c}{d} \frac{1}{1 \mp \sin\theta} \quad , \tag{1}$$

where c, d and θ denote the speed of light in vacuum, the period along the direction of the incident electric field and the angle of the incident THz waves, respectively. For the period of Px=700 μm, the first Rayleigh minimum appears at the frequency of 0.43 THz. Whereas, the localized resonant mode due to the slot aperture is determined by the equation

$$f_c = \frac{c}{2L} . \tag{1}$$

For L=600 μm, we can expect that the resonant peak appears near f_c=0.25 THz, under the condition of a perfect electric conductor.

A finite-difference time-domain (FDTD) method was used for our simulations. Periodic boundary conditions are applied in the directions, x and y, in the structure plane and perfect matched layers are defined in z direction.[14] In the THz frequencies, most metals can be considered as a perfect electric conductor. We therefore used the complex dielectric constant of aluminum, extracted by using the Drude model, even though we made the samples with stainless steel plates for our experiments.[32] By using the numerical simulations, we obtained zero-order transmission spectra, near electric-field and current density distributions in the sample surface.

We also fabricated the samples based on the designed structures. The perforated slots were arranged on a square lattice with the area of 20 cm by 20 cm. The diameter of the incident THz beam is quite smaller than the sample area and therefore any collective behavior in the structure is well captured. The samples were fabricated by using a femtosecond laser machining method, which is based on laser ablation performed by amplified femtosecond pulses. Laser ablation based on a pulsed laser enables to ablate material from a solid without thermal damages. This ensures the fabrication of the samples with well-constructed structures. The standard deviation values of the line edge roughness (LER) of the perforated slots are roughly less than 5 μm, which is up to two orders of magnitude less than the THz wavelengths of interest, as shown in the insets of Fig. 2.

For measuring the THz transmission spectra, we used a standard THz time-domain spectroscopy with a spectral range from 50 GHz to 2 THz.[33-36] Generating and detecting the transmitted THz radiation are based on a p-type InAs emitter and a photoconductive antenna, respectively. By using a blank cell made of a 2 cm by 2 cm square hole punctured on a piece of aluminum as a reference box, we measured the reference signals. We then measured the transmission spectra with the samples which are right on top of the reference box. Our experimental system provides the time-resolved traces of the transmitted THz electric fields. After carrying out fast Fourier transformations, we obtain information on both spectral amplitudes and phases. The normalization was carried out simply over the entire frequency by dividing the spectral amplitude of the transmitted THz waves by one of the reference signal.

3. RESULTS AND DISCUSSIONS

First, we measured the transmission spectra for two types of the samples as shown in the insets of Fig. 2(a) and 2(b). For realizing the three-dimensional subwavelength confinement, we designed the structure of complicated slot apertures, which has six-fold rotational symmetry as shown in the inset of Fig 2(a). We wanted to check out the polarization independence on the THz transmission in the structure. Figure 2(a) shows the transmission spectra measured by varying the polarization of the incident THz waves. The localized resonant peaks appear near the frequency of 0.21 THz, which corresponds to the cut-off frequency of a straight slot with the length of L=600 μm. In this case, the ends of the slots act as nodal points of electric field formed inside the apertures. Therefore, the peaks appearing at the frequency of 0.21 THz correspond to the fundamental mode supporting a half wavelength of the surface THz waves. The second resonant peaks due to the standing wave supporting one and a half wavelength also appear near the frequency of 0.79 THz. All the resonant peaks are angle-independent. However, in the case of sample B, as increasing the polarization of the incident

THz waves, the peak value is rapidly decreased as shown in Fig .2(b). In order to further analyze the property of the polarization independence, we compared the peak values extracted from the measured transmission spectra for the two samples as shown in Fig .2(c). At the 0° polarization, the two samples show almost the transmission efficiency whereas, at the 90° polarization, the peak value of the transmission spectra through sample B is rapidly decreased up to zero.

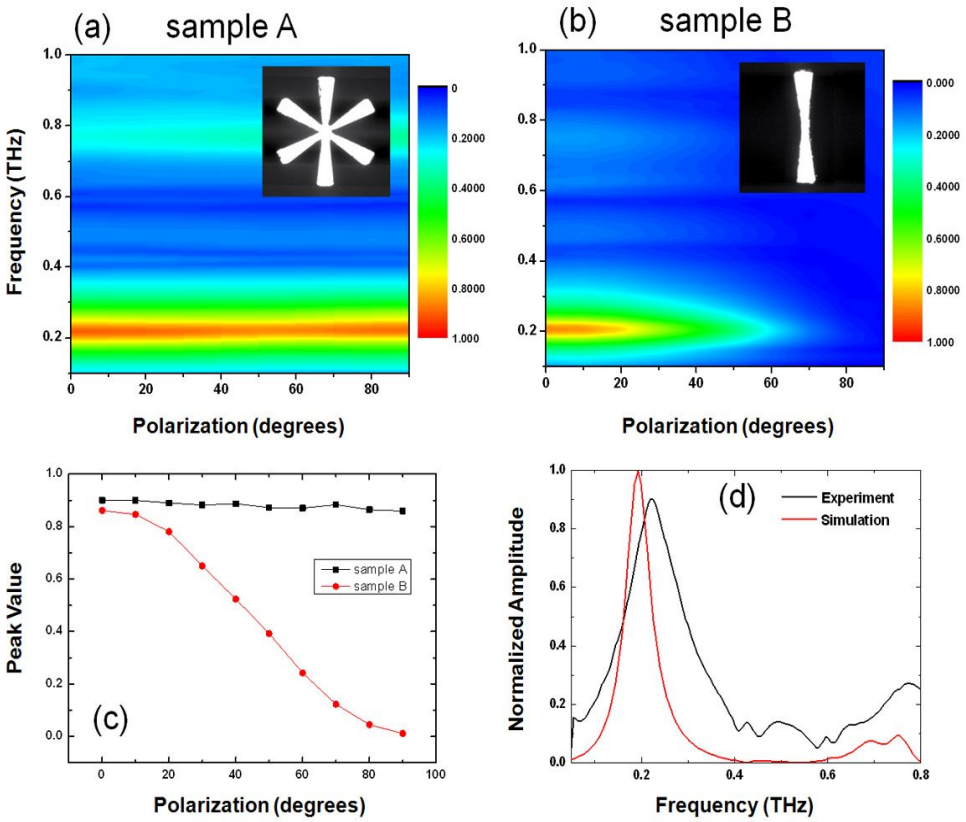

Figure 2. Normalized polarization-dependent transmission amplitudes for two types of the samples, shown in the insets, (a) sample A and (b) sample B. (c) Peak values extracted from the measured transmission spectra plotted versus the polarization of the incident THz radiation. (d) Measured (black curve) and simulated (red curve) transmission spectra of Sample A at 0° polarization.

As shown in Fig. 2(d), the peak value of the simulated transmission spectrum appears at the frequency of 0.2 THz. This is slightly lower than the measured peak value appearing at the frequency of 0.21 THz. However, the overall trend agrees well with the numerical simulation.

Figure 3 shows the results of numerical simulations showing the polarization-independent subwavelength confinement of THz surface waves. The simulations were carried out at the resonant frequency. Figure 3(a) shows the intensity of electric near-field distribution at the 0° polarization in the normal incidence case. The polarization is along the x-axis and therefore one slot among three in the sample structure is exactly parallel with the polarization. We therefore cannot observe the electric near-field distribution contributed by the slot parallel to the polarization. In the case of the 90° polarization, a slot among three in the sample structure is exactly perpendicular to the polarization. Therefore, the electric near-field distribution mainly appears on the slot perpendicular to the polarization, as shown in Fig. 3(b). The patterns of the electric near-field distributions, shown in Fig. 3(a) and 3(b), are a little bit difference, but the THz electric fields are strongly concentrated near the center of the structure in the sample.

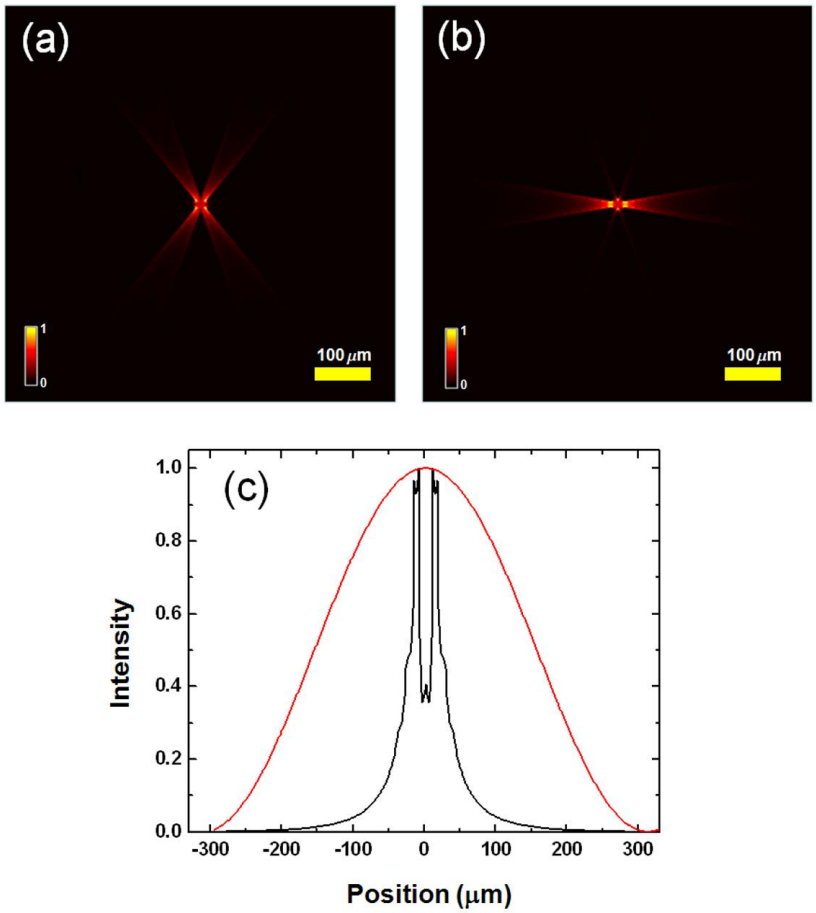

Figure 3. The intensities of electric near-field distributions on the xy plane at (a) 90° polarization and (b) at 0° polarization. (c) The intensity profile of the electric near field in the cross-section at the center of the sample. The red curve presents the square of the cosine function which wavelength is proportional to twice the length of a slot in the sample structure.

To further understanding the polarization-independent three dimensional subwavelength confinement of the THz electric fields, we plotted the intensity of the electric near field along the center axis of the structure for the case at 90° polarization, as shown in the black curve in Fig. 3(c). We can find two sharp concentrations of the THz electric field near the center of the structure. For comparison, we also plotted the square of cosine function corresponding to the resonant wavelength of twice the length of each slot, as shown in the red curve in Fig. 3(c). We therefore say that the THz electric field is concentrated near the center of the slots. The strong subwavelength confinement is also observed in any polarization.

4. CONCLUSIONS

In conclusion, we have achieved the polarization-independent three dimensional subwavelength confinement of THz surface waves. To realize that, we have used a coupled slot structure which consists of three perforated slots crossed at a single position to have six-fold rotational symmetry. Our experimental results have shown that the transmission is polarization-independent. Our theoretical simulations have additionally revealed that the confinement phenomenon appears in any polarization at the complicated structure of the slots. Finally, we have shown that the plasmonic structures with the functions of both the polarization independence and the three-dimensional subwavelength confinement can be designed. The understanding provides the possibility for designing and developing new types of plasmonic metamaterials with specific functionalities and photonic devices based on the structures.

5. ACKNOWLEDGEMENTS

This research was supported by Basic Science Research Program through the National Research Foundation of Korea (NRF) funded by the Ministry of Education, Science and Technology (2010-0021181, 2010-0025701) and by the APRI Research Program of GIST.

REFERENCES

[1] Ebbesen, T. W., Lezec, H. J., Ghaemi, H. F., Thio, T., and Wolff, P. A., "Extraordinary optical transmission through sub-wavelength hole arrays," Nature (London) 391, 667-669 (1998).
[2] Barnes, W. L., Dereux, A., and Ebbesen, T. W., "Surface plasmon subwavelength optics," Nature (London) 424, 824-830 (2003).
[3] Maier, S. A., Kik, P. G., Atwater, H. A., Meltzer, S., Harel, E., Koel, B. E., and Requicha, A. G., "Local detection of electromagnetic energy transport below the diffraction limit in metal nanoparticle plasmon waveguides," Nature Mater. 2, 229-232 (2003).
[4] Oulton, R. F., Sorger, V. J., Genov, D. A., Pile, D. F. P., and Zhang, X., "A hybrid plasmonic waveguide for subwavelength confinement and long range propagation," Nature Photon. 2, 496-500 (2008).
[5] Ozbay, E., "Plasmonics: Merging photonics and electronics at nanoscale dimensions," Science 311, 189-193 (2006).
[6] Nie, S. and Emory, S. R., "Probing single molecules and single nanoparticles by surface enhanced Raman scsttering," Science 275, 1102 (1997).
[7] Maier, S. A., Andrews, S. R., Martín-Moreno, L. and García-Vidal, F. J., "Terahertz surface plasmon polariton propagation and focusing on periodically corrugated metal wires," Phys. Rev. Lett. 97, 176805 (2006).
[8] Kawano, Y. and Ishibashi, K., "An on-chip near-field terahertz probe and detector," Nature Photon. 2, 618-621 (2008).
[9] Yoshida, H., Ogawa, Y., Kawai, Y., Hayashi, S., Hayashi, A., Otani, C., Kato, E., Miyamaru, F., and Kawase, K., "Terahertz sensing method for protein detection using a thin metallic mesh," Appl. Phys. LEtt. 91, 253901 (2007).
[10] Bingham, C. M., Tao, H., Liu, X., Averitt, R. D., Zhang, X., Padilla, W. J., "Planar wallpaper group metamaterials for novel terahertz applications," Opt. Express 16, 18565-18575 (2008).
[11] Pendry, J.B., S. R., Martín-Moreno, L. and García-Vidal, F. J., "Mimicking surface plasmons with structured surfaces," Science 305, 847-848 (2004).
[12] García-Vidal, F. J., S. R., Martín-Moreno, and Pendry, J.B., "Surfaces with holes in them: new plasmonic metamaterials," J. Opt. A Oure Aool. Opt. 7, S97 (2005).
[13] Seo, M. A., Park, H. R., Koo, S. M., Park, D. J., Kang, J. H., Suwal, O. K., Choi, S. S., Planken, P. C. M., Park, G. S., Park, N. K., Park, Q. H., and Kim, D. S., "Terahertz field enhancement by a metallic nano slit operating beyond the skin-depth limit," Nature Photon. 3, 152-156 (2009).
[14] Yang, J. K., Kee, C. S., and Lee, J. W., "Three-dimensional subwavelength confinement of terahertz electromagnetic surface modes in a coupled slit structure," Opt. Express 19, 20119-20204 (2011).
[15] Devilez, A., Bonod, N., Wenger, J., Gérard, D., Stout, B., Rigneault, H., and Popov, E., "Three-dimensional subwavelength confinement of light with dielectric microspheres," Opt. Express 17, 2089-2094 (2009).
[16] Seo, M. K., Kwon, S. H., Ee, H. S., and Park, H. G., "Full three-dimensional subwavelength high-Q surface plasmon polariton cavity," Nano Lett. 9, 4078-4082 (2009).
[17] Zhu, X. L., Ma, Y., Zhang, J. S., Xu, J., Wu, X. F., Zhang, Y., Han, X. B., Fu, Q., Liao, Z. M., Chen, L., and Yu, D. P., "Confined three-dimensional plasmon modes inside a ring-shaped nanocavity on a silver film imaged by cathodoluminescence microscopy," Phys. Rev. LEtt. 105, 127402 (2010).
[18] Chen, L., Shakya, J., and Lipson, M., "Subwavelength confinement in an integrated metal slot waveguide on silicon," Opt. Lett. 31, 2133-2135 (2006).
[19] Zhan, H., Mendis, R., and Mittleman, D. M., "Superfocusing terahertz waves below λ/250 using plasmonic parallel-plate waveguides," Opt. Express 18, 9643-9650 (2010).
[20] Chen, C. Y., Tsai, M. W., Chuang, T. H., Chang, Y. T., and Lee, S. C., "Effect of Wood's anomalies on the profile of extraordinary transmission spectra through metal periodic arrays of rectangular subwavelength holes with different aspect ratio," Appl. Phys. Lett. 91, 063108 (2007).

[21] Liu, X., Starr, T., Starr, A. F., and Padilla, W. J., "Infrared spatial and frequency selective metamaterials with near-unity absorbance," Phys. Rev. Lett. 104, 207403 (2010).
[22] Zhang, Z., Chan, K. T., Cui, Y., He, S., Wang, C., Xing, Q., and Wang, Q., "Multimode transmission in complementary plasmonic structures at terahertz frequencies," Appl. Phys. Lett. 96, 073506 (2010).
[23] Qiang, R., Chen, J., Zhao, T., Wang, S., Ruchhoeft, P., Morgan, M., "Modeling of infrared bandpass filters using a three-dimensional FDTD method," Electr. Lett. 41, 914-915 (2005).
[24] Imhof, C. and Zengerle, R., "Pairs of metallic crosses as a left-handed metamaterials with improved polarization properties," Opt. Express 14, 8257-8262 (2006).
[25] Lin, L., Hande, L. B., and Roberts, A., "Resonant nanometric cross-shaped apertures: Single apertures versus periodic arrays," Appl. Phys. Lett. 95, 201116 (2009).
[26] Thompson, P. G., Biris, C. G., Osley, E. J., Gaathon, O., Osgood, R. M., Panoiu, N. C., and Warburton, P. A., "Polarization-induced tenability of localized surface plasmon resonances in arrays of sub-wavelength cruciform apertures," Opt. Express 19, 25035-25047 (2011).
[27] Lin, L. and Roberts, A., "Angle-robust resonances in cross-shaped aperture arrays," Appl. Phys. Lett. 97, 061109 (2010).
[28] Roberts, A. and Lin, L., "Plasmonic quarter-wave plate," Opt. Lett. 37, 1820-1822 (2012).
[29] Liu, X., Tyler, T., Starr, T., Starr, A. F., Jokerst, N. M., and Padilla, W. J., "Taming the blackbody with infrared metamaterials as selective thermal emitters," Phys. Rev. Lett. 107, 045901 (2011).
[30] Aydin, K., Ferry, V. E., Briggs, R. M., and Atwater, H. A., "Broadband polarization-independent resonant light absorption using ultrathin plasmonic super absorbers," Nat. Commun. 2, 517 (2011).
[31] Niederer, G., Nakagawa, W., Herzig, H. P., and Thiele, H., "Design and characterization of a tunable polarization-independent resonant grating filter," Opt. Express 13, 2196-2200 (2005).
[32] D. Y. Smith, E. Shiles, and M. Inokuti, Handbook of Optical Constant of Solids, E. D. Palik, ed. (Academic, Orlando, Fla., 1985).
[33] Lee, J. W. and Kim, D. S., "Relative contribution of geometric shape and periodicity to resonant terahertz transmission," J. Appl. Phys. 107, 113109 (2010).
[34] Exter, M. V. and Grischkowsky, D., "Optical and electric properties of doped silicon from 0.1 to 2 THz," Appl. Phys. Lett. 56, 1694-1696 (1990).
[35] Jiang, Z., Li, M., Zhang, X. C., "Dielectric constant measurement of thin films by differential time domain spectropcopy," Appl. Phys. Lett. 76, 3221-3223 (2000).
[36] Zhao, G., Schouten, R. N., van der Valk, N., Wenckebach, W. T., and Planken, P. C. M., "Design and performance of a THz emission and detection setup based on a semi-insulation GaAs emitter," Rev. Sci. Instrum. 73, 1715-1719 (2002).